

PAPER • OPEN ACCESS

## A topological flux trap: Majorana bound states at screw dislocations

To cite this article: Stefan Rex and Roland Willa 2022 *New J. Phys.* **24** 053057

View the [article online](#) for updates and enhancements.

You may also like

- [Degeneracy of Majorana bound states and fractional Josephson effect in a dirty SNS junction](#)  
S Ikegaya and Y Asano
- [Majorana fermions in semiconductor nanowires: fundamentals, modeling, and experiment](#)  
T D Stanescu and S Tewari
- [Magneto-Josephson effects and Majorana bound states in quantum wires](#)  
Falko Pientka, Liang Jiang, David Pekker et al.



## PAPER

# A topological flux trap: Majorana bound states at screw dislocations

## OPEN ACCESS

## RECEIVED

22 December 2021

## REVISED

4 March 2022

## ACCEPTED FOR PUBLICATION

28 March 2022

## PUBLISHED

1 June 2022

Original content from  
this work may be used  
under the terms of the  
[Creative Commons  
Attribution 4.0 licence](#).

Any further distribution  
of this work must  
maintain attribution to  
the author(s) and the  
title of the work, journal  
citation and DOI.

Stefan Rex<sup>1,2,4</sup> and Roland Willa<sup>2,3,4,\*</sup><sup>1</sup> Institute for Quantum Materials and Technologies, Karlsruhe Institute of Technology, Karlsruhe, Germany<sup>2</sup> Institute for Theory of Condensed Matter, Karlsruhe Institute of Technology, Karlsruhe, Germany<sup>3</sup> Heidelberg Academy of Sciences, Heidelberg, Germany

\* Author to whom any correspondence should be addressed.

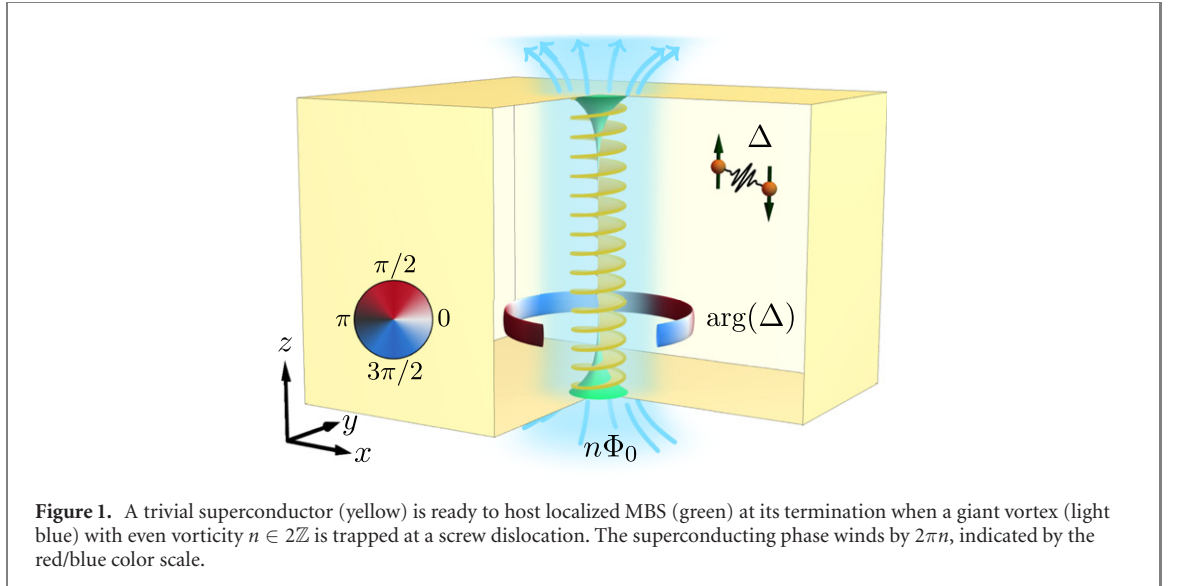
<sup>4</sup> These two authors contributed equally.E-mail: [roland.willa@kit.edu](mailto:roland.willa@kit.edu)**Keywords:** topology, vortices, superconductivity, Majorana bound statesSupplementary material for this article is available [online](#)

## Abstract

The engineering of non-trivial topology in superconducting heterostructures is a very challenging task. Reducing the number of components in the system would facilitate the creation of the long-sought Majorana bound states. Here, we explore a route toward emergent topology in a trivial superconductor without a need for other proximitized materials. Specifically, we show that a vortex hosting an even number of flux quanta is capable of forming a quasi-one-dimensional topological sub-system that can be mapped to the Kitaev wire, if the vortex is trapped at a screw dislocation. This crystallographic defect breaks inversion symmetry and thereby threads a local spin-orbit coupling through the superconductor. The vortex-dislocation pair in the otherwise trivial bulk can harbor a pair of Majorana bound states located at the two surface terminations. We explain the topological transition in terms of a band inversion in the Caroli-de Gennes-Matignon vortex bound states and discuss favorable material parameters.

## 1. Introduction

Majorana bound states (MBS) are self-conjugate, non-abelian quasi-particles that appear as boundary modes in topological superconductors [1, 2]. The foreseen applications of MBS in quantum computation [3] have motivated tremendous effort to generate them in a variety of systems, yet without conclusive evidence. To date, the design of Majorana platforms largely relies on the paradigm of proximity: owed to the sparsity of intrinsic topological superconductors, non-trivial topology is engineered in heterostructures, e.g., in semiconductor nanowires [4, 5] with partial [6–11] or full [12] superconducting shell or at superconductors interfacing with topological insulators [13, 14]. The recurring key components are spin-orbit coupling, Zeeman splitting, and (trivial) *s*-wave superconductivity. Here we take a different approach, where these components readily coexist without proximity effects and may cause the formation of a topological phase. The surprisingly simple system consists of a trivial superconductor in an external magnetic field, where a vortex is trapped at a screw dislocation. Screw dislocations are well understood and commonly occurring crystallographic defects, which introduce a spin-orbit coupling by locally breaking inversion symmetry [15]. While MBS at vortices usually require a *p*-wave superconductor [2], we show below that this symmetry restriction can be lifted if the vortex carries multiple flux quanta [12, 16]. Depending on their type, superconductors tend to carry magnetic field either through large normal-state regions (type-I) or vortices with singly-quantized flux  $\Phi_0 = hc/2e$  (type-II). Yet, the formation of *giant vortices*, carrying a flux  $n\Phi_0$ ,  $|n| \gtrsim 1$  is known to occur under appropriate circumstances [17]. Generally, Caroli-de Gennes-Matignon (CdGM) states [18] at sub-gap energies are found close to the vortex line. Including the effect of Zeeman splitting, an inversion of the CdGM bands is possible. We show that this inversion turns the vortex-dislocation system into an effective topological wire with MBS at the surface terminations. We thus demonstrate that, in principle, MBS can arise from a trivial superconductor, i.e., a



superconductor where the 3D bulk does not possess nonzero topological indices in the absence of other adjacent materials.

We first introduce a minimal model and argue that MBS are symmetry-allowed for an even number of flux quanta. We then demonstrate the conceptual reduction of the system to a quasi-one-dimensional Majorana wire. Finally, we consider in more detail the spatial profile of multi-flux (giant) superconducting vortices and their CdGM states for vorticities  $n > 1$  and discuss suitable conditions to enter the topological regime.

## 2. Model and symmetries

Consider a screw dislocation along the  $z$  axis trapping a giant vortex with  $n$  flux quanta in an  $s$ -wave superconductor. Around the  $s$  axis, the phase of the superconducting order parameter winds by  $2\pi n$  and we assume a pairing gap of the form  $\Delta(\mathbf{r}) = \Delta_0(r)e^{-in\varphi}$  in cylindrical coordinates. Schematically, the setup is shown in figure 1.

In the Nambu basis  $\Psi = (\Psi_\uparrow, \Psi_\downarrow, \Psi_\downarrow^\dagger, -\Psi_\uparrow^\dagger)^T$ , the electronic system is described by the Bogoliubov-de Gennes (BdG) Hamiltonian

$$\mathcal{H}_{\text{BdG}}(\mathbf{r}) = \begin{pmatrix} H_0(\mathbf{r}) + H_{\text{soc}}(\mathbf{r}) & \Delta(\mathbf{r})\sigma_0 \\ \Delta^*(\mathbf{r})\sigma_0 & -\sigma_y[H_0^*(\mathbf{r}) + H_{\text{soc}}^*(\mathbf{r})]\sigma_y \end{pmatrix} \quad (1)$$

with the electronic contribution

$$H_0(\mathbf{r}) = (\mathbf{p} + e\mathbf{A}/c)^2/2m - E_F - g\mu_B\mathbf{B} \cdot \boldsymbol{\sigma}/2, \quad (2)$$

and spin-orbit contribution [15]

$$H_{\text{soc}}(\mathbf{r}) = \alpha(r)(p_z/\hbar)[\cos(p_z a/2\hbar)\sigma_y - i \sin(p_z a/2\hbar)\sigma_x] \quad (3)$$

imposed by the screw winding. Here, we have the momentum operator  $\mathbf{p} = -i\hbar\nabla$ , the electron charge  $-e < 0$ , the period length  $a$  of the screw dislocation, the Fermi energy  $E_F$ , the gyromagnetic ratio  $g$ , and the Bohr magneton  $\mu_B$ . The magnetic field  $\mathbf{B}$  relates to the vector potential  $\mathbf{A}$  via  $\mathbf{B} = \nabla \times \mathbf{A}$ . The Pauli matrices  $\boldsymbol{\sigma} \equiv (\sigma_x, \sigma_y, \sigma_z)^T$  act in spin space, while those acting in the particle-hole space are denoted with  $\tau_{x,y,z}$ . In compounds with high ionicity, the role of  $\sigma_x$  and  $\sigma_y$  in equation (3) may be exchanged as shown in reference [15]. This modification has no implications on our following arguments.

The Hamiltonian possesses the particular rotational symmetry  $[\mathcal{H}_{\text{BdG}}, J_z] = 0$ , with the modified angular momentum operator  $J_z \equiv -i\hbar\partial_\varphi + (n/2)\tau_z$ , which accounts for the vorticity  $n$ . Note that the translation along  $z$  by the distance  $a$  (as part of the screw operation) has been omitted in  $J_z$  as it does not affect the topological regime, see supplementary material <https://stacks.iop.org/NJP/24/053057/mmedia> [19]. The eigenvalue  $\ell$  of  $J_z$  is a good quantum number and the eigenfunctions of  $\mathcal{H}_{\text{BdG}}$  may be labeled as

$$\Psi_\ell(r, \varphi, z) = \psi_\ell(r, z)e^{i[\ell - (n/2)\tau_z]\varphi}. \quad (4)$$

The constraint  $\ell - (n/2) \in \mathbb{Z}$  assures that the wave functions remain single-valued under a circulation around the giant vortex,  $\varphi \rightarrow \varphi + 2\pi$ . This yields integer (half-integer) values for  $\ell$  when  $n$  is even (odd).

As a minimal requirement, MBS must be eigenstates of the particle-hole operator  $\mathcal{C} = \tau_y \sigma_y \mathcal{K}$ , with  $\mathcal{K}$  the complex conjugation. Since the particle-hole operator anti-commutes with the modified angular momentum,  $\{\mathcal{C}, J_z\} = 0$ , it holds  $\ell \mapsto -\ell$  under  $\mathcal{C}$ . Consequently, any MBS must have  $\ell = 0$  to be mapped onto itself. Together with the single-valuedness of  $\Psi_\ell$ , it follows that  $n \in 2\mathbb{Z}$  is a *necessary* condition for the existence of MBS. Similar arguments are known from full-shell nanowires [12] and magnetic skyrmions [16, 20], and go back to earlier work on vortex-bound zero modes [21]. The system of bound-states centered around the vortex core can be assigned the same topological  $\mathbb{Z}_2$  index as multi-mode quantum wires [22–25], see supplementary material [19]. However, topological transitions can only be triggered by a band inversion of modes with  $\ell = 0$ . To gain more qualitative insight, the problem is reduced to a one-dimensional effective problem in the following.

### 3. Reduction to one dimension

The angular dependence can be removed from the problem by virtue of the unitary transformation

$$U_J \equiv e^{-i[\ell - (n/2)\tau_z]\varphi}. \quad (5)$$

This motivates us to narrow the following discussion to the subspace of even vorticity  $n$  and  $\ell = 0$ . Neglecting the radial dependence of  $\alpha(r)$  on the scale of the giant vortex, the wave function decomposes into  $\psi_0(r, z) = \psi_0(z)\chi(r)$ , with a scalar radial part  $\chi(r)$  and an axial part  $\psi_0(z)$ . While the separation of variables helps to streamline our analysis, the assumption on  $\alpha$  must be relaxed in most real materials, where the Thomas–Fermi length is shorter than the superconducting coherence length. At the same time, our qualitative findings are robust toward a decaying shape of  $\alpha(r)$  as long as the net spin–orbit effect on the relevant CdGM wavefunctions does not vanish. For the CdGM states, which have energies well inside the bulk gap  $\Delta_\infty$ ,  $\chi(r)$  is localized at the vortex. Here, we neglect all other states to study the low-energy properties of the system. To capture the emergence of MBS, it is convenient to average out the radial dependence and obtain an effective one-dimensional problem along the  $z$  axis. Let the probability-weighted planar mean for a quantity  $X(r)$  be

$$\langle X(r) \rangle_\chi = \int_0^\infty dr r \chi^\dagger(r) X(r) \chi(r). \quad (6)$$

The mean radius  $R = \langle r \rangle_\chi$ , superconducting gap  $\bar{\Delta} = \langle \Delta_0(r) \rangle_\chi$ , and field strength  $\bar{B} = \langle B(r) \rangle_\chi$  are of particular interest here. Furthermore, the mean Zeeman splitting  $\bar{E}_Z = g\mu_B \bar{B}/2$  is introduced for brevity. Note that even in the presence of in-plane anisotropy, a reduction to a low-energy 1D model of vortex bound states is possible, if an appropriate form factor  $f(\varphi)$  is introduced in the planar average. After a spin-space rotation with  $U_\sigma = \exp[i\sigma_z k_z a/4]$ , the effective low-energy 1D Hamiltonian reads

$$H_{\text{eff}} = \left[ \frac{\hbar^2 k_z^2}{2m} - \bar{\mu} \right] \tau_z - \bar{E}_Z \sigma_z + \alpha k_z \tau_z \sigma_y + \bar{\Delta} \tau_x, \quad (7)$$

with an effective chemical potential  $\bar{\mu} \ll E_F$  [19]. By virtue of equation (7), the electronic states within the vortex/dislocation tube are described by the well-known Hamiltonian of Majorana nanowires, which enters the topological phase for [4, 5]

$$\bar{E}_Z^2 > |\bar{\Delta}|^2 + \bar{\mu}^2, \quad (8)$$

i.e., for sufficiently large effective field strength  $\bar{B}$ . In this phase, MBS appear at the ends of the wire, that is at the two surface terminations of the vortex/dislocation axis. Remarkably, this demonstrates that the system at hand—a trivial superconductor—is generically susceptible to a topological regime with MBS. To solidify this conceptual result, we give more details on the nature of the transition and suitable material properties below.

### 4. Giant vortices and CdGM states

The spatial distribution of the superconducting order parameter  $\Delta$  and the magnetic vector potential  $\mathbf{A}$  is well captured within the Ginzburg–Landau (GL) theory. In reduced units, see references [26, 27] and the supplementary material [19], the free energy density

$$\mathcal{F}_{\text{GL}} = \frac{\kappa^2}{4} (|\Delta|^2 - 1)^2 + \frac{1}{2} |(\nabla + i\mathbf{A})\Delta|^2 + \frac{1}{2} (\nabla \times \mathbf{A})^2 \quad (9)$$

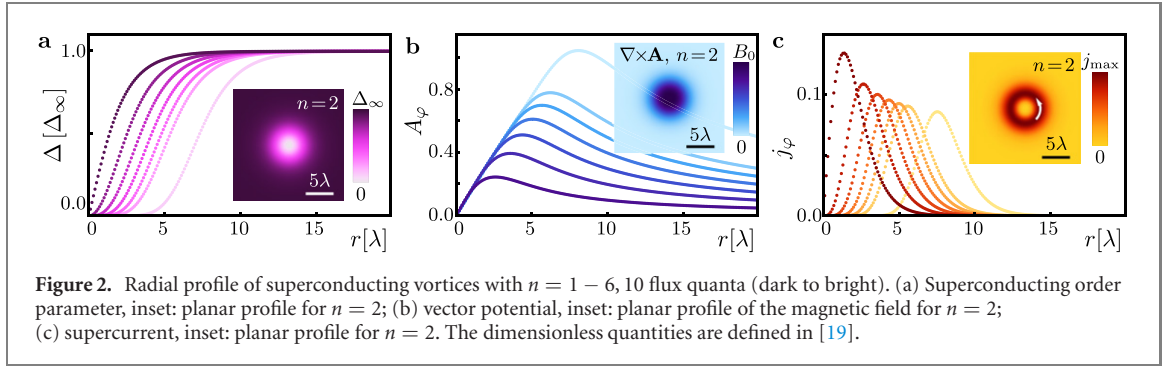


**Figure 2.** Radial profile of superconducting vortices with  $n = 1 - 6, 10$  flux quanta (dark to bright). (a) Superconducting order parameter, inset: planar profile for  $n = 2$ ; (b) vector potential, inset: planar profile of the magnetic field for  $n = 2$ ; (c) supercurrent, inset: planar profile for  $n = 2$ . The dimensionless quantities are defined in [19].

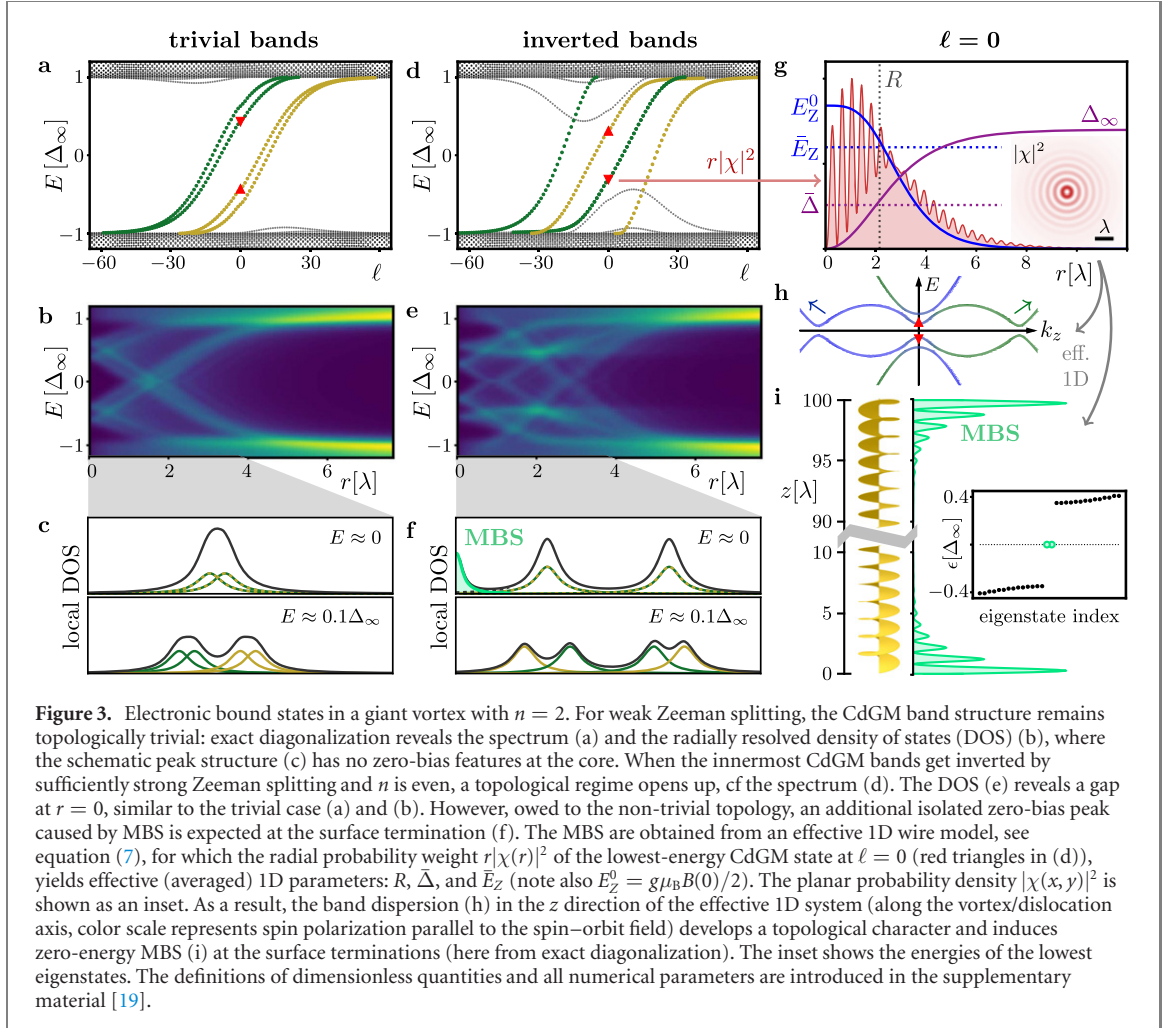


**Figure 3.** Electronic bound states in a giant vortex with  $n = 2$ . For weak Zeeman splitting, the CdGM band structure remains topologically trivial: exact diagonalization reveals the spectrum (a) and the radially resolved density of states (DOS) (b), where the schematic peak structure (c) has no zero-bias features at the core. When the innermost CdGM bands get inverted by sufficiently strong Zeeman splitting and  $n$  is even, a topological regime opens up, cf the spectrum (d). The DOS (e) reveals a gap at  $r = 0$ , similar to the trivial case (a) and (b). However, owed to the non-trivial topology, an additional isolated zero-bias peak caused by MBS is expected at the surface termination (f). The MBS are obtained from an effective 1D wire model, see equation (7), for which the radial probability weight  $r|\chi(r)|^2$  of the lowest-energy CdGM state at  $\ell = 0$  (red triangles in (d)), yields effective (averaged) 1D parameters:  $R$ ,  $\bar{\Delta}$ , and  $\bar{E}_Z$  (note also  $E_Z^0 = g\mu_B B(0)/2$ ). The planar probability density  $|\chi(x, y)|^2$  is shown as an inset. As a result, the band dispersion (h) in the  $z$  direction of the effective 1D system (along the vortex/dislocation axis, color scale represents spin polarization parallel to the spin-orbit field) develops a topological character and induces zero-energy MBS (i) at the surface terminations (here from exact diagonalization). The inset shows the energies of the lowest eigenstates. The definitions of dimensionless quantities and all numerical parameters are introduced in the supplementary material [19].

is solely characterized by the dimensionless quantity  $\kappa = \lambda/\xi$ , the ratio of the superconducting penetration depth  $\lambda$  and the coherence length  $\xi$ . Taking full account of the dislocation, the screw symmetry imposes a staircase winding of the supercurrent. However, as shown by Ivlev and Thompson [28], this effect is parametrically small in  $a/\lambda$ , and shall be neglected here. The parameter  $\kappa$  is decisive of whether a superconductor is of type-I ( $\kappa < \kappa_c \equiv 1/\sqrt{2}$ ) or type-II ( $\kappa > \kappa_c$ ). Close to  $\kappa_c$ , the vortex-vortex interactions become small, allowing for stable giant vortices with intermediate vorticities.

Numeric vortex solutions in the weak type-I case ( $\kappa = 0.4$ ), figure 2, define the confining normal-core  $\Delta(\mathbf{r})$ , vector potential  $A(\mathbf{r})$ , and current  $\mathbf{j}(\mathbf{r})$  relevant for electronic CdGM states. Let us stress that type-I superconductors of finite thickness are ready to host vortices with a low number of flux quanta [17]. In fact, *single-flux* vortices become stable below a threshold thickness  $\sim \xi/(1 - \kappa/\kappa_c)$ . Close to  $\kappa_c$ , this mesoscopic length bridges from the microscopic scales of the superconductor to the macroscopic lengths in bulk specimen. Furthermore, the screw dislocation provides an additional pinning potential, see [19]. Note that a weak type-II superconductor with a strong pinning potential at the dislocation line would be an equally

suitable candidate for our proposal. This gives us good reason to believe that the existence of giant vortices trapped at dislocation lines should persist to specimens of macroscopic size.

The confinement of electrons by the superconducting flux tube provides discrete CdGM in-gap states that crucially depend on the vorticity [18, 29–33]. These states are obtained by solving the BdG Hamiltonian (1) in the plane orthogonal to the vortex axis (recall  $\alpha(r)$  is assumed constant within the vortex region). Figures 3(a)–(f) shows the spectrum of CdGM states and the corresponding density of states. In absence of Zeeman splitting, the CdGM states disperse as a function of the (discrete) quantum number  $\ell$  and a total of  $|n|$  spin-degenerate branches cross zero energy [33]. As derived in reference [32], these states have a typical spacing  $\Delta E \approx (\Delta_\infty^2/E_F) \frac{\pi^2 |n|^{1-\gamma}}{2\pi+4|n|^\gamma}$ , with  $\Delta_\infty$  the asymptotic superconducting energy gap and  $\gamma$  a non-universal exponent close to unity (reference [32] reports  $\gamma \approx 0.78$ ). Flux tubes with an odd vorticity feature a large number of low-energy states at small  $|\ell|$ . Giant vortices with an even number of flux quanta, on the contrary, have a large energy gap of the order of  $\Delta_\infty$  at  $\ell = 0$ . Combining these two results one arrives at a crude, yet surprisingly accurate, estimate for the separation  $\Delta\ell \approx 2(E_F/\Delta_\infty)/|n|^{1-\gamma}$  between branch crossings as a function of the modified angular momentum  $\ell$ .

## 5. Topology and Majorana bound states

Including the Zeeman effect, the spin degeneracy is lifted and each branch splits into a pair of non-degenerate branches (in the two-fold redundant BdG formalism), with clear signatures in the local density of states. Upon increasing the splitting, the two branches closest to zero energy at  $\ell = 0$  get inverted, which corresponds to the topological transition captured by equation (8): the CdGM spectrum at  $\ell = 0$  maps approximately to the spectrum of the one-dimensional Hamiltonian with averaged fields, equation (7), at  $k_z = 0$ . In figure 3, both the trivial CdGM (a)–(c) and inverted (topological) bands (d)–(f) are shown. A mapping to an effective 1D wire is achieved by radial averaging, see figure 3(g) and [19] for details. The inversion of the lowest two states indicates the gap closing and reopening known from Majorana wires, see figure 3(h) for the dispersion relation for the inverted-band case. Note that only the central CdGM bands of the 1D system matter for the topological phase and could, in principle, be directly mapped to the Kitaev chain [1] without the detour to the nanowire model. However, to make the role of the spin–orbit coupling more apparent we keep a four-band effective model. The radial averaging (6) bears several advantages. On the one hand, it formally maps a higher-dimensional problem to a 1D effective model, see equation (7), which is readily identified with the topological nanowire. In the supplementary material we provide a detailed argument that the topological character is independent of this reduction scheme. On the other hand, the numerical solution of the problem is now split in two tasks: first, the vortex core and CdGM states are computed for the radial problem, figures 3(a)–(g). In the second stage, the effective parameters allow to solve the nano-wire problem, figures 3(h) and (i). Both tasks can be performed with high numerical accuracy. The full two-dimensional exact diagonalization calculations in the  $rz$ -plane—a task that becomes necessary if the spin–orbit coupling shows a strong spatial dependence—would impose severe numerical limitations on the system size, and the results would be overly prone to finite-size errors.

In the topological phase, MBS appear at the terminations of the wire, i.e. one at each sample surface. The CdGM states can be resolved in the differential conductance of scanning tunneling experiments [34], as shown schematically in figures 3(c) and (f). A MBS would lead to an *additional* peak located at  $E = 0$  and close to  $r = 0$ . Such a peak—unattached to the dispersive CdGM bands—is a measurable signature of the MBS. The relative strength of this peak in comparison to the other subgap states depends on the localization of the MBS at the surface. The probability density of the MBS along the  $z$  axis is shown in figure 3(i). The characteristic length  $\zeta \approx v_F/\Delta_{\text{eff}}$  of the exponential localization  $\propto e^{-z/\zeta}$  is inversely proportional to the effective gap  $\Delta_{\text{eff}}$  in 1D. The latter may be given by the band gap at either  $k_z = 0$  or  $k_z \approx k_F$  with the Fermi wave vector  $k_F$  of the effective wire.

## 6. Material requirements

Before concluding, let us briefly comment on the energy scales involved in the problem, and how they cooperate to favor a topological phase: the five independent energy scales to consider here are (i) the kinetic energy  $K = \hbar^2/2m\xi^2$  at wavelengths  $\sim \xi$ , depending on the *effective* mass  $m$ , (ii) the Fermi energy  $E_F$  (iii) the bulk superconducting gap  $\Delta_\infty$ , (iv) the Zeeman splitting  $\bar{E}_Z$ , and (v) the spin–orbit splitting  $\alpha k_F$  induced by the screw dislocation. Apart from natural constants, the Zeeman splitting only depends on the superconducting penetration depth,  $\bar{E}_Z \propto \lambda^{-2}$  (assuming  $\kappa \approx 1$ ), and is estimated to be in the range 10 – 100  $\mu\text{eV}$  for typical values of  $\lambda$ . To reach the topological regime, the spacing of the lowest CdGM states

at  $\ell = 0$  must not exceed the Zeeman energy. At the same time, the superconducting gap  $\Delta_\infty$  needs to be large enough to allow for measurements. As the spacing between CdGM branches decreases with  $K$ , a large effective mass would facilitate the band inversion. Furthermore,  $E_F/\Delta_\infty$  should be moderate to ensure an unambiguous resolution of the MBS zero-energy peak. Also, our effective low-energy model is only valid for a small Fermi energy. This is again favored by a large effective mass. Spin–orbit effects enter the game once band inversion is present: opening a substantial gap at  $k_z = k_F$  reduces the localization length  $\zeta$  and avoids the hybridization of the two MBS. Spin–orbit coupling is guaranteed by the dislocation [15]; the strength depends on the chemical composition of the material and will likely increase for heavier elements. Whereas our approximation of a radially constant parameter  $\alpha(r) \approx \alpha$  requires the Thomas–Fermi length to be comparable to the coherence length, relaxing the approximation will not qualitatively affect the findings, but merely add quantitative constraints. In summary, we expect our proposal to apply to superconductors with  $\kappa \approx 1$ , large effective mass  $m$ , not too strong superconducting gap  $\Delta_\infty$  and a crystal system known to host screw dislocations. Suitable giant vortices can be created by sweeps of an external magnetic field.

Identifying a specific material that fulfills all of the requirements above is a challenging task that goes beyond the scope of this work. Although we cannot predict a strong candidate, we conclude our discussion with a brief prospect on relevant material classes for future investigations related to our conceptual proposal. We focus on two key properties: the capability to host multi-quantum vortices and a small Fermi energy. The former by itself is not too difficult. With a rapidly increasing number of reported compounds [35–38], finding superconductors at the type-I/type-II-crossover is very realistic. Alternatively, giant vortices can be created in type-II superconductors by means of lateral specimen confinement and control of vortex pinning [39–42]. Exceptionally small Fermi levels, on the other hand, have recently been reported in iron-based compounds such as FeSe [43, 44]. In addition, there is a growing family of superconducting-doped semiconductors [45] with members of both type-I and type-II. Such materials frequently have unconventional properties that are absent in our model, and doping would also require to account for disorder effects. More specialized models combined with DFT results may help to find a good candidate in future work.

## 7. Conclusion

We demonstrated that a pair of topological lines—a giant vortex trapped at a screw dislocation—is capable of creating a quasi-one-dimensional topological wire hosting MBS in an otherwise trivial superconductor. This proposal now awaits physical realization, which—unlike other defect-based systems, e.g. [46]—is facilitated by the trivial bulk topology of the superconducting state. Screw dislocations are ubiquitous and their appearance can often be controlled during sample growth. Giant vortices, on the other hand, are known to exist in easily available materials. Therefore, our proposal opens an exciting and realistic route to hunt for MBS without sophisticated fabrication of nano-hybrid structures, such that topological superconductivity may become accessible for a broad experimental community.

## Acknowledgments

We are extremely grateful to T Gozliniski, Q Li, and W Wulfhekel, who provided the initial spark to this project and challenged it with critical interactions and discussions. We thank V B Geshkenbein, I V Gornyi, F Hassler, R P Huebener, A D Mirlin, and J Schmalian for useful discussions. SR was supported by the Deutsche Forschungsgemeinschaft via the Grant No. MI 658/12-1 (joint DFG-RFBR project) and No. MI 658/13-1 (joint DFG-RSF project). RW acknowledges funding support from the Heidelberg Academy through its WIN initiative (8. Teilprogramm).

## Data availability statement

The data that support the findings of this study are available upon reasonable request from the authors.

## References

- [1] Kitaev A Y 2001 Unpaired Majorana fermions in quantum wires *Phys.-Usp.* **44** 131
- [2] Ivanov D A 2001 Non-abelian statistics of half-quantum vortices in p-wave superconductors *Phys. Rev. Lett.* **86** 268
- [3] Nayak C, Simon S H, Stern A, Freedman M and Das Sarma S 2008 Non-abelian anyons and topological quantum computation *Rev. Mod. Phys.* **80** 1083
- [4] Oreg Y, Refael G and von Oppen F 2010 Helical liquids and Majorana bound states in quantum wires *Phys. Rev. Lett.* **105** 177002

- [5] Lutchyn R M, Sau J D and Das Sarma S 2010 Majorana fermions and a topological phase transition in semiconductor-superconductor heterostructures *Phys. Rev. Lett.* **105** 077001
- [6] Mourik V, Zuo K, Frolov S M, Plissard S R, Bakkers E P A M and Kouwenhoven L P 2012 Signatures of Majorana fermions in hybrid superconductor-semiconductor nanowire devices *Science* **336** 1003
- [7] Deng M T, Yu C L, Huang G Y, Larsson M, Caroff P and Xu H Q 2012 Anomalous zero-bias conductance peak in a Nb–InSb nanowire–Nb hybrid device *Nano Lett.* **12** 6414
- [8] Das A, Ronen Y, Most Y, Oreg Y, Heiblum M and Shtrikman H 2012 Zero-bias peaks and splitting in an Al–InAs nanowire topological superconductor as a signature of Majorana fermions *Nat. Phys.* **8** 887
- [9] Rokhinson L P, Liu X and Furdyna J K 2012 The fractional a.c. Josephson effect in a semiconductor–superconductor nanowire as a signature of Majorana particles *Nat. Phys.* **8** 795
- [10] Deng M T, Vaitiekėnas S, Hansen E B, Danon J, Leijnse M, Flensberg K, Nygård J, Krogstrup P and Marcus C M 2016 Majorana bound state in a coupled quantum-dot hybrid-nanowire system *Science* **354** 1557
- [11] Gül Ö *et al* 2018 Ballistic Majorana nanowire devices *Nat. Nanotechnol.* **13** 192
- [12] Vaitiekėnas S *et al* 2020 Flux-induced topological superconductivity in full-shell nanowires *Science* **367** 6485
- [13] Fu L and Kane C L 2008 Superconducting proximity effect and Majorana fermions at the surface of a topological insulator *Phys. Rev. Lett.* **100** 096407
- [14] Xu J-P *et al* 2015 Experimental detection of a Majorana mode in the core of a magnetic vortex inside a topological insulator-superconductor  $\text{Bi}_2\text{Te}_3/\text{NbSe}_2$  heterostructure *Phys. Rev. Lett.* **114** 017001
- [15] Hu L *et al* 2018 Ubiquitous spin–orbit coupling in a screw dislocation with high spin coherency *Phys. Rev. Lett.* **121** 066401
- [16] Rex S, Gornyi I V and Mirlin A D 2019 Majorana bound states in magnetic skyrmions imposed onto a superconductor *Phys. Rev. B* **100** 064504
- [17] Huebener R P 2001 *Magnetic Flux Structures in Superconductors* 2nd edn (Berlin: Springer)
- [18] Caroli C, de Gennes P G and Matricon J 1964 Bound fermion states on a vortex line in a type II superconductor *Phys. Lett.* **9** 307
- [19] see supplementary material (<https://stacks.iop.org/NJP/24/053057/mmedia>).
- [20] Yang G, Stano P, Klinovaja J and Loss D 2016 Majorana bound states in magnetic skyrmions *Phys. Rev. B* **93** 224505
- [21] Volovik G E 1999 Fermion zero modes on vortices in chiral superconductors *JETP* **70** 609
- [22] Potter A C and Lee P A 2010 Multichannel generalization of Kitaev’s Majorana end states and a practical route to realize them in thin films *Phys. Rev. Lett.* **105** 227003
- [23] Lutchyn R M, Stanescu T D and Das Sarma S 2011 Search for Majorana fermions in multiband semiconducting nanowires *Phys. Rev. Lett.* **106** 127001
- [24] Tewari S and Sau J D 2012 Topological invariants for spin–orbit coupled superconductor nanowires *Phys. Rev. Lett.* **109** 150408
- [25] Samokhin K V 2020 Majorana modes in multiband superconducting quantum wires *Phys. Rev. B* **101** 094502
- [26] Blatter G, Feigel’man M V, Geshkenbein V B, Larkin A I and Vinokur V M 1994 Vortices in high-temperature superconductors *Rev. Mod. Phys.* **66** 1125
- [27] Palonen H, Jäykkä J and Paturi P 2013 Giant vortex states in type I superconductors simulated by Ginzburg–Landau equations (arXiv:1308.3661)
- [28] Ivlev B I and Thompson R S 1991 Exotic vortices for spiral-layered superconductors *Phys. Rev. B* **44** 12628
- [29] Tanaka Y, Hasegawa A and Takayanagi H 1993 Energy spectrum of the quasiparticle in a quantum dot formed by a superconducting pair potential under a magnetic field *Solid State Commun.* **85** 321
- [30] Tanaka K, Robel I and Jankó B 2002 Electronic structure of multiquantum giant vortex states in mesoscopic superconducting disks *Proc. Natl Acad. Sci. USA* **99** 5233
- [31] Virtanen S M M and Salomaa M M 1999 Multiquantum vortices in superconductors: electronic and scanning tunneling microscopy spectra *Phys. Rev. B* **60** 14581
- [32] Berthod C 2005 Vorticity and vortex-core states in type-II superconductors *Phys. Rev. B* **71** 134513
- [33] Volovik G E 1993 Vortex motion in Fermi superfluids and the Callan–Harvey effect *JETP Lett.* **57** 244
- [34] Yin J-X, Pan S H and Hasan M Z 2021 Probing topological quantum matter with scanning tunnelling microscopy *Nat. Rev. Phys.* **3** 249
- [35] Sun S, Liu K and Lei H 2016 Type-I superconductivity in  $\text{KBi}_2$  single crystals *J. Phys.: Condens. Matter.* **28** 085701
- [36] Singh J, Jayaraj A, Srivastava D, Gayen S, Thamizhavel A and Singh Y 2018 Possible multigap type-I superconductivity in the layered boride  $\text{RuB}_2$  *Phys. Rev. B* **97** 054506
- [37] Peets D C, Cheng E, Ying T, Kriener M, Shen X, Li S and Feng D 2019 Type-I superconductivity in  $\text{Al}_6\text{Re}$  *Phys. Rev. B* **99** 144519
- [38] Garcia-Campos P, Huang Y K, de Visser A and Hasselbach K 2021 Visualization by scanning SQUID microscopy of the intermediate state in the superconducting Dirac semimetal  $\text{PdTe}_2$  *Phys. Rev. B* **103** 104510
- [39] Grigorieva I V, Escoffier W, Misko V R, Baelus B J, Peeters F M, Vinnikov L Y and Dubonos S V 2007 Pinning-induced formation of vortex clusters and giant vortices in mesoscopic superconducting disks *Phys. Rev. Lett.* **99** 147003
- [40] Cren T, Serrier-Garcia L, Debontridder F and Roditchev D 2011 Vortex fusion and giant vortex states in confined superconducting condensates *Phys. Rev. Lett.* **107** 097202
- [41] Ge J-Y, Gladilin V N, Tempere J, Xue C, Devreese J T, Van de Vondel J, Zhou Y and Moshchalkov V V 2016 Nanoscale assembly of superconducting vortices with scanning tunnelling microscope tip *Nat. Commun.* **7** 13880
- [42] Golod T, Pagliero A and Krasnov V M 2019 Two mechanisms of Josephson phase shift generation by an Abrikosov vortex *Phys. Rev. B* **100** 174511
- [43] Coldea A I and Watson M D 2018 The key ingredients of the electronic structure of  $\text{FeSe}$  *Annu. Rev. Condens. Matter Phys.* **9** 125
- [44] Huang W, Lin H, Zheng C, Yin Y, Chen X and Ji S-H 2021 Superconducting  $\text{FeSe}$  monolayer with millielectronvolt Fermi energy *Phys. Rev. B* **103** 094502
- [45] Bustarret E 2015 Superconductivity in doped semiconductors *Physica C* **514** 36
- [46] Chen C, Jiang K, Zhang Y, Liu C, Liu Y, Wang Z and Wang J 2020 Atomic line defects and zero-energy end states in monolayer  $\text{Fe}(\text{Te}, \text{Se})$  high-temperature superconductors *Nat. Phys.* **16** 536